Effect of Annealing on the Characteristics of Organic Solar Cells: Polymer Blends with a 2-Vinyl-4,5-dicyanoimidazole Derivative

Thomas Kietzke,*,† Richard Yee Cheong Shin,† Daniel Ayuk Mbi Egbe,‡ Zhi-Kuan Chen,† and Alan Sellinger†

Institute of Materials Research and Engineering (IMRE), 3 Research Link, Republic of Singapore 117602, Institute of Organic Chemistry and Macromolecular Chemistry of the Friedrich-Schiller-University Jena, Humboldtstrasse. 10, D-07743 Jena, Germany

Received March 15, 2007; Revised Manuscript Received March 26, 2007

ABSTRACT: Photovoltaic cells based on blends of either regioregular poly(3-hexylthiophene-2,5-diyl) (P3HT) or a poly(phenylenevinylene) (A-PPE-PPV) derivative as electron donors with a novel electron acceptor based on 2-vinyl-4,5-dicyanoimidazole (Vinazene) have been investigated in detail. We found a strong influence of annealing conditions on the thin-film nanostructure and device performance. By adjusting the material combinations, external quantum efficiencies between 12 and 15% and energy conversion efficiencies of 0.5% could be reached. Though comparable efficiencies with both donor polymers could be obtained with the Vinazene derivative as acceptor, we found strong indications that different mechanisms are limiting the device efficiency.

Introduction

Organic solar cells have attracted tremendous attention by promising low-cost large-area solar cells.[1,2] Of the two competing technologies to process organic solar cells, vacuum and solution, solution processing is considered most promising as it allows for high throughput processes like reel-to-reel, screen, and ink jet printing. By blending and solution processing regioregular poly(3-hexylthiophene-2,5-diyl) (P3HT) as electron donor and the fullerene derivative 6,6-phenyl-C61-butyric acid methyl ester (PCBM) as electron acceptor, organic solar cells with energy conversion efficiencies of 5% were recently demonstrated under simulated sun light.[3,4] Despite the promising efficiencies obtained for the P3HT:PCBM devices, this system has several drawbacks: First, P3HT:PCBM based solar cells generate a low open circuit voltage of only 0.65−0.70 V. This low open circuit voltage is one of the major loss mechanisms in this system, taking into account that only photons with energies exceeding the optical band gap of P3HT of 1.9 eV are absorbed. A higher open circuit voltage exceeding 1 V would be desirable to allow for direct driving of low-power electronic devices like calculators and watches without requiring any additional serial connections. Second, the absorbance coefficient of PCBM in the visible region is relatively low, such that the photoresponse of the P3HT:PCBM devices is mainly due to the P3HT absorption alone. Third, fullerenes in general and PCBM in particular, are prepared and purified using very sophisticated fabrication technologies, making them rather expensive and thus not the first choice for low-cost solar cells.

In an effort to find lower-cost materials to replace fullerene derivatives, a novel electron acceptor based on 2-vinyl-4,5-dicyanoimidazole[5] (termed Vinazene) was synthesized in high yield by a two-step process from commercially available materials. Here we present a detailed study on the influence of annealing conditions on the morphology and photovoltaic performance of P3HT and poly(2,5-dioctyloxy-1,4-phenylene-ethynylene-9,10-anthracenylene-ethynylene-2,5-dioctyloxy-1,4-phenylene-vinylene-2,5-di(2′-ethyl)hexyloxy-1,4-phenylene-vinylene **(**A-PPE-PPV) with 4,7-bis(2-(1-hexyl-4,5-dicyanoimidazol-2-yl)vinyl)benzo[c]1,2,5-thiadiazole (V-BT).

* Corresponding author. E-mail: thomas.kietzke@web.de.
† Institute of Materials Research and Engineering.
‡ Institute of Organic Chemistry and Macromolecular Chemistry of the Friedrich-Schiller-University Jena.

Results and Discussion

The synthesis of V-BT shown in Figure 1 is described elsewhere.[6] The energy of the lowest unoccupied molecular orbital (LUMO) and highest occupied molecular orbital (HOMO) are −3.49 and −5.87 eV, respectively. V-BT is highly soluble in common polar solvents like chloroform, acetone, or chlorobenzene and has a melting temperature of 205 °C with no observable glass transition temperature (T_g).

For solar cells, a broad spectral absorbance is desired in order to harvest as much solar radiation as possible. Because the acceptor V-BT absorbs mainly between 300 and 500 nm, we chose A-PPE-PPV[7] and P3HT, two donor polymers (chemical structures shown in Figure 1) that exhibit strong absorption properties in the complementary wavelength region from 500 to 650 nm.

As shown in the thin film absorbance spectra in Figure 2a, A-PPV-PPE and V-BT absorb in nearly complementary spectral regions, making this combination a promising candidate for efficient light harvesting. The 1:1 blend of both materials absorb a substantial portion of the visible spectrum between 300 and 625 nm. After photoexcitation of an electron from the HOMO to the LUMO, the electron can jump from the LUMO of the donor (the material with the higher LUMO) to the LUMO of the acceptor if the potential difference of the ionization potential of the donor and the electron affinity of the acceptor is larger than the exciton binding energy. Typical exciton binding energies in conjugated polymers are estimated to be around 300 meV. The LUMO energy of A-PPE-PPV is −3.1 eV. Thus the LUMO of V-BT (−3.49 eV) is sufficiently lower that photogenerated excitons on A-PPE-PPV have a chance to be separated at the heterointerface. In addition, the offset of the LUMO of V-BT of the HOMO of A-PPE-PPV (−5.20 eV) is sufficiently large that high open-circuit voltages can be expected.

Blend layers were spin-coated from solutions of A-PPE-PPV (M_w: 36 000 g/mol, PDI = 3.00 as determined by GPC) and

10.1021/ma0706273 CCC: $37.00
Published on Web 06/02/2007

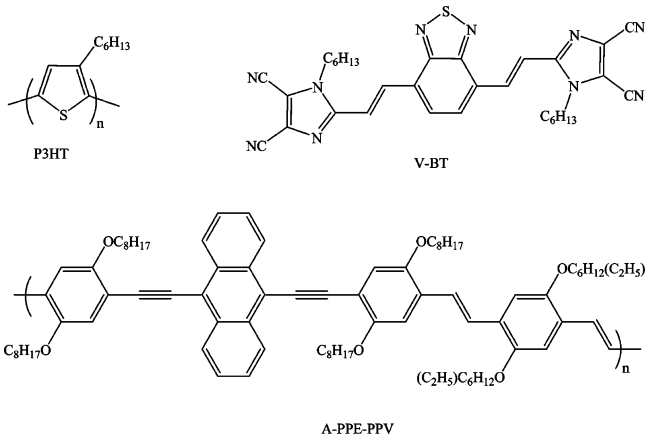

Figure 1. Chemical structures of P3HT, V-BT, and A-PPE-PPV.

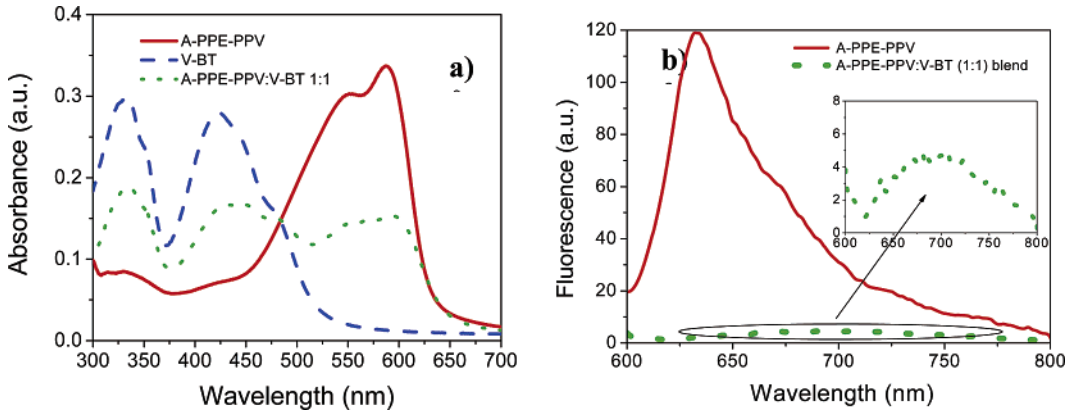

Figure 2. (a) Absorbance spectra of a layer of A-PPE-PPV (solid line), of V-BT (dashed), and of a 1:1 mixture by weight of V-BT and A-PPE-PPV (dotted line). (b) Corresponding photoluminescence spectra recorded at an excitation wavelength of 580 nm (upper figure).

V-BT in chloroform (5 mg/mL of each material, 1 wt % solutions) on glass slides for optical studies or on glass:ITO:PEDOT:PSS substrates for solar cell devices. Photoluminescence spectra of the blend layer and of the individual single components were recorded to investigate the degree of luminescence quenching in the blend system.

The photoluminescence of A-PPE-PPV upon excitation at 580 nm (excitation of A-PPE-PPV only) is nearly completely quenched, as shown in Figure 2b, indicating an effective charge transfer of the photogenerated electron on A-PPE-PPV to the V-BT molecules. Interestingly, a residual broad featureless red-shifted emission centered around 700 nm was observed. We attribute this peak to an exciplex formed between A-PPE-PPV and V-BT, similar to reports on exciplex formation in blends of donor/acceptor PPV derivatives.[8,9] Further studies on the origin of this broad red-shifted emission are under investigation.

In the next step, solar cell devices using A-PPE-PPV:V-BT as active layers were prepared and the incident-photon-to-current-efficiency (IPCE) was measured. The IPCE is a measure of the external quantum efficiency and is defined as:

$$\mathrm{IPCE} = \frac{\text{no. of electrons}}{\text{no. of photons}} = \frac{hcI_{\mathrm{SC}}}{e\lambda P_{\mathrm{light}}}$$

where λ is the incident wavelength, I_{SC} the short-circuit current, e the elementary charge, h the Planck constant, c the speed of light, and P_{light} the incident light power.

We investigated different weight ratios and found that highest efficiencies could be obtained for a 1:1 by weight blend of A-PPE-PPV:V-BT. We found that the as-prepared (without annealing) device exhibited a rather low IPCE of <3%. This low efficiency is rather surprising because the PL measurements described before indicated an efficient separation of the photogenerated exciton. Most likely a percolation path for the separated charge carriers to their corresponding electrodes is absent. This would adversely affect the transport properties, as indicated by the low fill factor. In addition, the observed exciplex emission indicates that recombination of the dissociated charge carriers in the vicinity of the heterointerface might represent a major loss path.

Because it is well-known that postannealing of the active layers often leads to increased device performance of polymer blend-based organic solar cells,[9,10] we studied the influence of annealing on the efficiency for this system. After annealing the active layer prior to cathode deposition at 80 °C for 10 min, a device efficiency of 12.2% was obtained, a 4× improvement of nonannealed devices (see Figure 3). Under white light illumination (AM 1.5, 100mW/cm^2), we measured an energy conversion efficiency (ECE) of 0.42% with a corresponding fill factor of 35%. Furthermore, a rather high open-circuit voltage (V_{OC}) of 0.98 V was observed for the annealed devices, roughly 200 meV higher than what is reported for A-PPE-PPV:PCBM blend devices.[7] The higher open-circuit voltage can be explained because less energy is lost when the photogenerated electrons transfer from the A-PPV-PPE to the V-BT (LUMO −3.49 eV) than to PCBM (LUMO −3.8 eV).

The increased efficiency after annealing can be attributed to a change in the thin-film nanostructure. To confirm this, we recorded atomic force microscopy (AFM) images for the as-prepared devices annealed at different temperatures, as shown in Figure 4. The as prepared layer exhibits a fine scale

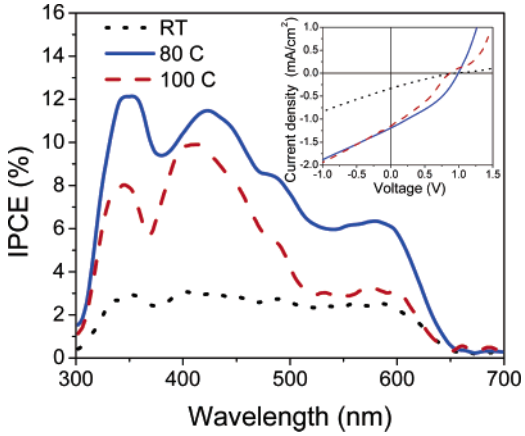

Figure 3. (a) IPCE spectra for A-PPE-PPV:V-BT blend devices annealed at different temperatures. The inset shows the corresponding $I(V)$ characteristics.

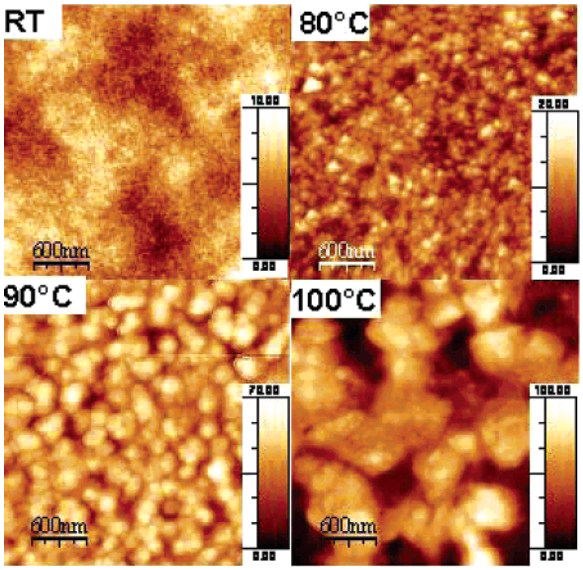

Figure 4. AFM topology images of the A-PPE-PPV:V-BT blend layers as prepared and after annealing at different temperatures as indicated for 10 min, the height scale is measured in nm.

phase separation in the nanometer range. This fine phase separation enables efficient dissociation of the photogenerated excitons at the heterointerface, as proven by the nearly complete PL quenching. However, most likely, a percolating path for the separated charge carriers is missing. Thus only few charge carriers can be extracted, whereas most recombine again, limiting the device efficiency. After annealing at 80 °C, the phase separation increases, but the film appears to be homogeneously mixed with feature sizes in the few tens of nanometers. Since the phase separation is still in the range of the exciton diffusion length, which is estimated for conjugated polymers to be between 5 and 20 nm, most photogenerated excitons can still reach the heterointerface. Because of the larger domains, it is now more likely for the separated charge carriers to reach the electrodes, hence the device efficiency is much higher.

However, the 100 °C annealed layer is characterized by large agglomerates extending over several hundreds of nanometers with accompanied high surface roughness. The domains are now much bigger than the exciton diffusion length. As there was no clear T_g found for the A-PPV-PPE, most likely the V-BT molecules diffuse at temperatures around 80 °C in the A-PPE-PPV matrix and begin to aggregate (Table 1).

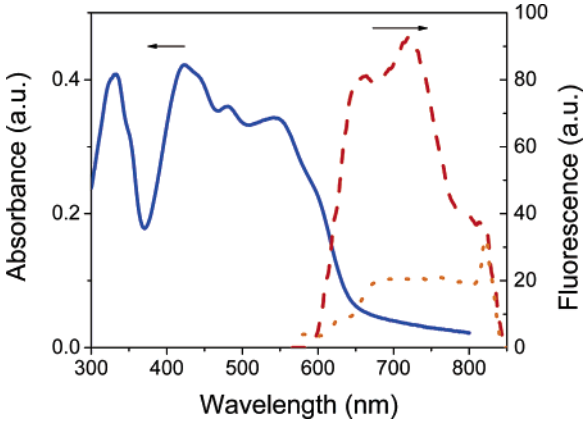

Figure 5. Absorbance spectrum of a P3HT:V-BT (1:1) blend (solid line) and PL spectra of a P3HT layer (dashed line) and of the P3HT:V-BT (1:1) blend on glass (dotted line) at an excitation wavelength of 520 nm.

Table 1. Characteristic Parameters for A-PPE-PPV:V-BT Blend Solar Cells under AM 1.5 Illumination for the As-Prepared Device (RT) and after Annealing at 80 and 100 °C

annealing T	I_{sc} (mA)	FF (%)	V_{oc} (V)	ECE (%)	IPCE (%)
RT	0.35	21	0.94	0.07	3.0
80 °C	1.20	35	0.98	0.42	12.2
100 °C	1.16	32	0.87	0.31	10.1

Most interestingly, a change in the shape of the IPCE spectra after annealing could be observed. Only for the as-prepared device, the IPCE spectrum follows the absorbance spectrum as shown in Figure 2a, whereas after annealing the IPCE spectrum is dominated by the characteristic absorption of V-BT in the wavelength region between 330 and 420 nm. This is particularly obvious if the spectra of the as-prepared and the 100 °C annealed devices are compared. In the region between 500 and 600 nm, the efficiency remains nearly unchanged, whereas the quantum efficiency at 350 nm increases from 3 to 12%. These observations can be explained by the formation of two different phases after annealing. One phase consists of nearly pure A-PPE-PPV, whereas the other one is V-BT rich with some fraction of A-PPE-PPV, quite similar to what is reported for blends of two polyfluorene derivatives.[11,12] Only in the V-BT rich phase, efficient charge separation and transport would take place (Figure 3).

For comparison, we also studied the performance of P3HT:V-BT solar cells. Initially, we varied the ratio of P3HT to V-BT from 2:1 to 1:3 (not shown here) and found that the 1:1 blend produced the optimum results. For the experiments, commercially available P3HT (Rieke Metals Inc., regioregularity 90−93%, M_w: 20 800 g/mol, PDI = 1.20 as determined by GPC) was used. Unlike for the A-PPV-PPE:V-BT blends, we found that 1:1 blends of P3HT:V-BT gave only partial quenching of P3HT fluorescence, indicating that charge separation of the photogenerated exciton is not very efficient (Figure 5). Most likely, the offset of the LUMO of P3HT (ca. −3.2 eV) and the LUMO of V-BT (−3.49 eV) is too low to separate the excitons, as reported for other organic solar cells.[13] Taking this into account, it is very surprising that the P3HT:V-BT solar cells still exhibit quite high external quantum efficiencies of about 15%. This is to our knowledge the highest efficiency reported for blends of P3HT with small molecules other than those based on fullerene derivatives.[14−16]

In contrast to the A-PPV-PPE-V-BT devices discussed before, the P3HT:V-BT devices exhibited a high quantum efficiency of 12% even without any annealing steps. Annealing at 120 °C

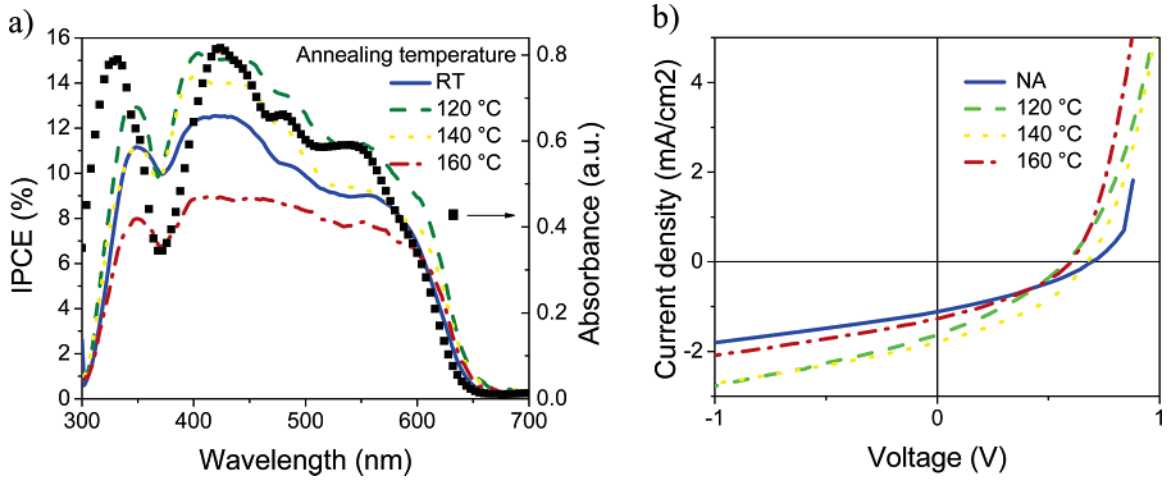

Figure 6. (a) IPCE spectra for P3HT:V-BT or the as-prepared blend layer on glass is shown. (b) Corresponding *I*(*V*) characteristics.

Table 2. Characteristic Parameters for P3HT:V-BT (1:1) Solar Cells under AM 1.5 Illumination

annealing T	I_{sc} (mA)	FF (%)	V_{oc} (V)	ECE (%)	IPCE (%)
RT	1.10	31.0	0.69	0.25	12
120 °C	1.64	31.4	0.58	0.31	15
140 °C	1.79	37.3	0.67	0.45	14
160 °C	1.27	31.0	0.61	0.26	9

could improve the quantum efficiency slightly further to 15%, as shown in Figure 6a. However, the IPCE spectra resembles largely the absorbance spectrum of the 1:1 blend for all investigated annealing conditions. This indicates that both materials contribute equally to the photocurrent.

Higher annealing temperatures again led to a decrease in the IPCE. However, regarding the energy conversion efficiency under white light illumination, annealing at 140 °C was the optimum temperature because a higher fill factor was reached. The fill factor increased slightly from 31% for the nonannealed device to a quite moderate fill factor of 37.3% after annealing at 140 °C. We attribute this increase to changes in the morphology, leading to better percolation properties (Figure 6).

To study the influence of the annealing temperature on morphology, AFM images were recorded for as-prepared and annealed layers at 120 and 140 °C (Table 2). As expected, the annealed films become more rough, indicating possible V-BT and P3HT crystallization. Because of the possible crystallization of P3HT, the interpretation of the AFM images are not as straightforward as for blends containing the amorphous A-PPV-PPE discussed before. To arrive at a clearer interpretation, we rinsed the layers with acetone to selectively remove the V-BT, as P3HT is not soluble in acetone while V-BT is. To our surprise, for the 120 °C annealed rinsed layers, we found a honeycomb-like structure for the remaining P3HT with pores of about 50 nm diameter. Upon higher annealing temperatures, the pore structure fused together to form worm-like structures. We propose that, upon annealing, rather pure regions of semicrystalline P3HT and crystalline V-BT are formed and a large fraction of V-BT protrudes to the surface layer and crystallizes, leading to the very rough surface as observed in AFM. The remaining V-BT is trapped in the honeycomb-like P3HT structures. Unfortunately, the structure sizes of 50 nm are larger than the exciton diffusion length (10−20 nm) such that many excitons recombine before reaching the heterointerface, thus limiting the efficiency. The dimension of the phase separation in the layer does not differ much after the different annealing steps compared to the not annealed device. This explains why annealing does not have a dramatic influence on the device efficiency compared to the A-PPV-PPE based devices (Figure 7).

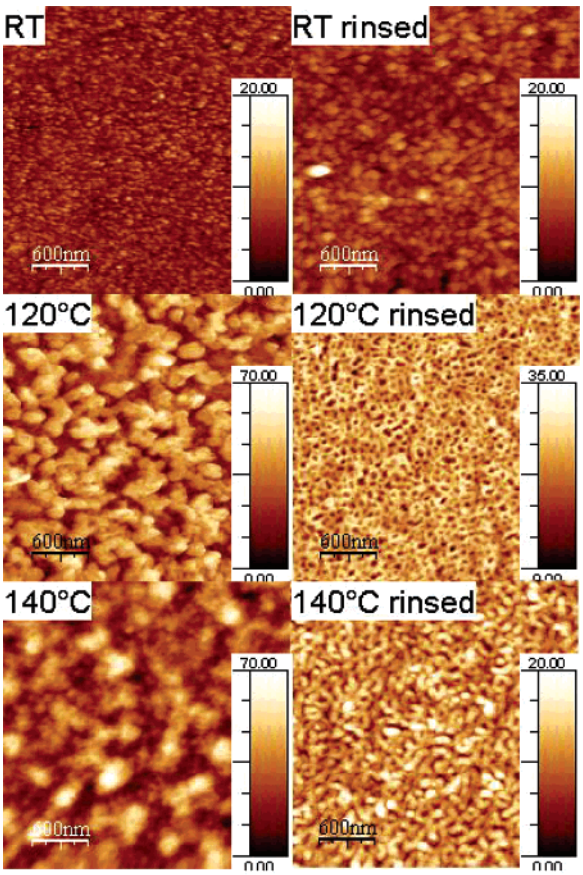

Figure 7. AFM topology images recorded for the as prepared (RT), at 120 °C and at 140 °C annealed P3HT:V-BT layers before and after rinsing with acetone; the height scale is measured in nm.

Summary

We present for the first time detailed studies on the influence of annealing on nanostructure and photovoltaic performance of A-PPE-PPV or P3HT blends with a novel Vinazene-based accepting small molecule, V-BT. Similar high external quantum efficiencies in the range of 12−15% could be reached for both donor materials after optimizing the annealing conditions. However, the efficiency limiting processes are rather different for each case. The efficiency in the P3HT:V-BT devices is

limited by incomplete dissociation of the photogenerated excitons as indicated by incomplete PL quenching. Conversely, the A-PPE-PPV:V-BT blends show nearly complete quenching and thus very efficient exciton separation. However, missing percolation pathways and recombination via exciplex emission seem to be the limiting processes. Further spectroscopic studies are needed to give more insight in these processes. The fill factor for each donor polymer blended with V−BT reached values between 30−40%, indicating that low electron mobility, as in the case of polymeric acceptors, may be the limiting factor preventing higher efficiencies. Measurements of the electron mobility are currently underway, and preliminary efforts have been made to increase the fill factor to 50% while doubling the efficiency using a modified version of V-BT, which will be the content of a future article.

Experimental Methods

Device Preparation. For device fabrication, an approximately 70 nm thick layer of poly(ethylene dioxythiophene) doped with polystyrene sulfonic acid (PEDOT:PSS) was spin-coated onto commercial glass substrates covered with indium-tin-oxide (polished 140 nm ITO on SiO_2 covered soda lime glass, Merck). The PEDOT:PSS (HC Starck) films were dried on a hot plate under a nitrogen atmosphere for 30 min at 120 °C. After spin-coating, the blend from chloroform solution (10 mg/mL) at 2000 revolutions per minute (rpm), the devices were annealed on a hot plate at the indicated temperatures. The devices were completed by evaporating a 20 nm Ca layer protected by 100 nm of Ag at a base pressure of 2×10^{-6} mbar. The effective solar cell area, as defined by the geometrical overlap between the bottom ITO electrode and the top cathode, was 0.1425 cm^2. The devices were prepared and characterized under nitrogen atmosphere.

Solar Cell Characterization. The IPCE as a function of wavelength was measured with a home-built setup consisting of an Oriel 300 W Xe lamp in combination with an Oriel Cornerstone 130 monochromator and a SRS 810 lock-in amplifier (Stanford Research Systems). The number of photons incident on the device was calculated for each wavelength by using a calibrated Si diode as reference. The white light measurements were performed using a solar simulator (Steuernagel, Germany model 535) and a Keithley 2400 source/measure unit.

Fluorescence Measurements. Steady-state fluorescence spectra were measured with a Perkin-Elmer LS 55 luminescence spectrometer. The excitation was incident at an angle of 60° on the glass surface, and the emission was recorded in reflection at an angle of 30° with respect to the surface normal.

Atomic Force Microscopy. AFM images were acquired with a Veeco multimode atomic force microscope in tapping mode. The cantilever (model NCR, Nanoworld AG) had a resonance frequency of 285 kHz, and the tip radius was specified to be less than 10 nm.

Acknowledgment. This research has been supported by the Agency for Science, Technology, and Research (A*STAR) and IMRE through the VIP Program in Organic Electronics coordinated by Prof. Ananth Dodabalapur. We thank Zi En Ooi and Lawrence Dunn for their technical assistance.

References and Notes

(1) Hoppe, H.; Sariciftci, N. S. *J. Mater. Res.* **2004**, *19*, 1924−1945.
(2) Gledhill, S. E.; Scott, J. C.; Gregg, B. A. *J. Mater. Res.* **2005**, *20*, 3167−3179.
(3) Ma, W.; Yang, C.; Gong, X.; Lee, K.; Heeger, A. J. *Adv. Funct. Mater.* **2005**, *15*, 1617−1622.
(4) Reyes-Reyes, M.; Kim, K.; Carroll, D. L. *Appl. Phys. Lett.* **2005**, *87*, 083506.
(5) Johnson, D. M.; Rasmussen, P. G. *Macromolecules* **2000**, *33*, 8597−8603.
(6) Shin, R. Y. C.; Kietzke, T.; Sudhakar, S.; Chen, Z. K.; Dodabalapur, A.; Sellinger, A. *Chem. Mater.* **2007**, *19*, 1892−1894.
(7) Hoppe, H.; Egbe, D. A. M.; Mühlbacher, D.; Sariciftci, N. S. *J. Mater. Chem.* **2004**, *14*, 3462−3467.
(8) Offermans, T.; van Hal, P. A.; Meskers, S. C. J.; Koetse, M. M.; Janssen, R. A. J. *Phys. Rev. B* **2005**, *72*, 045213−045211.
(9) Kietzke, T.; Neher, D.; Hörhold, H. H. *Chem. Mater.* **2005**, *15*, 6532−6537.
(10) Padinger, F.; Rittberger, R.; Sariciftci, N. S. *Adv. Funct. Mater.* **2003**, *13*, 1−4.
(11) Ramsdale, C. M.; Bache, I. C.; MacKenzie, J. D.; Thomas, D. A.; Arias, A. C.; Donald, A. M.; Friend, R. H.; Greenham, N. C. *Physica E* **2002**, *14*, 268−271.
(12) Stevenson, R.; Arias, A. C.; Ramsdale, C. M.; MacKenzie, J. D.; Richards, D. *Appl. Phys. Lett.* **2001**, *79*, 2178−2181.
(13) Kietzke, T.; Egbe, D. A. M.; Hörhold, H. H.; Neher, D. *Macromolecules* **2006**, *39*, 4018−4022.
(14) Shin, W. S.; Jeong, H. H.; Kim, M. K.; Jin, S. H.; Kim, M. R.; Lee, J. K.; Lee, W. L.; Gal, Y. S. *J. Mater. Chem.* **2006**, *16*, 384−390.
(15) Li, J.; Dierschke, F.; Wu, J.; Grimsdale, A. C.; Muellen, K. *J. Mater. Chem.* **2006**, *16*, 96−100.
(16) Camaioni, N.; Ridolfi, G.; Fattori, V.; Faveretto, L.; Barbarella, G. *J. Mater. Chem.* **2005**, *15*, 2220−2225.

MA0706273